Rhodopsin's Carboxy-Terminal Cytoplasmic Tail Acts as a Membrane Receptor for Cytoplasmic Dynein by Binding to the Dynein Light Chain Tctex-1

Andrew W. Tai,*‖ Jen-Zen Chuang,†‖
Christian Bode,‡ Uwe Wolfrum,‡
and Ching-Hwa Sung*†§
*Department of Cell Biology and Anatomy
†Department of Ophthalmology
Margaret M. Dyson Vision Research Institute
Weill Medical College of Cornell University
New York, New York 10021
‡Institut für Zoology
Johannes Gutenberg-Universität Mainz
D-55099 Mainz
Germany

Summary

The interaction of cytoplasmic dynein with its cargoes is thought to be indirectly mediated by dynactin, a complex that binds to the dynein intermediate chain. However, the roles of other dynein subunits in cargo binding have been unknown. Here we demonstrate that dynein translocates rhodopsin-bearing vesicles along microtubules. This interaction occurs directly between the C-terminal cytoplasmic tail of rhodopsin and Tctex-1, a dynein light chain. C-terminal rhodopsin mutations responsible for retinitis pigmentosa inhibit this interaction. Our results point to an alternative docking mechanism for cytoplasmic dynein, provide novel insights into the role of motor proteins in the polarized transport of post-Golgi vesicles, and shed light on the molecular basis of retinitis pigmentosa.

Introduction

Photoreceptors are highly polarized neurons (Figure 1A). The outer segment (OS) contains visual transduction proteins arranged in hundreds of stacked membrane disks. The OS is connected to the inner segment (IS) and cell body via a narrow nonmotile connecting cilium. Rhodopsin, the light-transducing visual pigment of rod cells, is synthesized in the proximal IS, yet is highly concentrated in the OS. Therefore, an efficient vectorial transport system must be required to deliver large numbers of newly synthesized rhodopsin molecules ($\sim10^7$ molecules per day per photoreceptor) to the base of the OS. Although the molecular basis of this directional trafficking is unclear, there is considerable immunocytochemical evidence that rhodopsin is vectorially transported through the IS to the OS in post-Golgi membrane vesicles. These vesicles dock and fuse with the apical IS membrane and rhodopsin is then incorporated into OS disk membranes (Papermaster et al., 1986).

Microtubule-based transport is an attractive candidate mechanism for the transport of rhodopsin in photoreceptors. In vertebrate photoreceptors, cytoplasmic microtubules nucleate from the basal body at the base of the connecting cilium (Figure 1A). In fish photoreceptors, these microtubules are oriented with uniform polarity with their minus ends facing the OS and plus ends facing the synaptic terminal (Troutt and Burnside, 1988). A similar microtubule organization is likely to be present in mammals, since the basal body is the only apparent microtubule organizing center in mammalian photoreceptors (Wolfrum, 1995). Therefore, the minus end–directed microtubule motor cytoplasmic dynein (Paschal et al., 1987) is a candidate motor for the transport of rhodopsin-laden vesicles across the IS to the base of the connecting cilium.

Each multisubunit cytoplasmic dynein complex consists of two heavy chains containing the ATPase and motor activities, two or three intermediate chains (DICs; 74 kDa), a group of light intermediate chains ($\sim$52–61 kDa; Gill et al., 1994), and one or more of each of the three recently described light chains (DLCs; 8 kDa, 14 kDa, and 22 kDa; King et al., 1996a, 1996b). DIC has been proposed to indirectly anchor dynein to its cargoes (Vallee et al., 1995) via binding to the dynactin complex (Karki and Holzbaur, 1995; Vaughan and Vallee, 1995). However, little is known about the identity of the "receptors" on the cargo membrane vesicles. The functions of the remaining subunits of cytoplasmic dynein are also poorly understood.

Several lines of evidence indicate that the carboxy-terminal cytoplasmic tail of rhodopsin encodes targeting signal(s) for its vectorial transport. This region is highly conserved among vertebrates and is a hot spot for mutations that cause some forms of retinitis pigmentosa (RP) (Macke et al., 1993; Sung et al., 1994), an inherited degenerative disease of photoreceptors that often leads to blindness (reviewed in Dryja and Li, 1995). Naturally occurring C-terminal mutant rhodopsins found in RP patients do not have significant defects in phototransduction (Sung et al., 1991b, 1994; Weiss et al., 1995). However, two of these C-terminal mutants (Q344ter and P347L) display a specific defect in transport to the OS in that they are mislocalized to the IS and cell body plasma membranes in transgenic photoreceptors, whereas endogenous wild-type rhodopsin remains OS localized (Sung et al., 1994; Li et al., 1998). In addition, rhodopsin C-terminal peptides block the formation of rhodopsin-bearing post-Golgi vesicles in a cell-free system (Deretic et al., 1998). Finally, this domain contains a novel cytoplasmic apical targeting determinant when expressed in polarized epithelial Madin–Darby canine kidney cells (Chuang and Sung, 1998).

By analogy to other protein transport systems, the targeting signal in rhodopsin's C-terminal cytoplasmic tail is likely to interact with intracellular sorting/transport machinery. In a search for proteins that interact with the C terminus of rhodopsin, we isolated a bovine ortholog of Tctex-1 (t complex testis expressed-1), which had

§To whom correspondence should be addressed (e-mail: chsung@mail.med.cornell.edu).
‖These authors contributed equally to this work.

A **B**
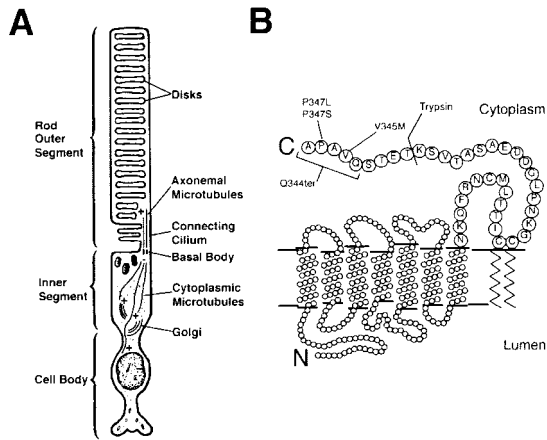
Figure 1. Rod Photoreceptor Morphology and Human Rhodopsin Topology

(A) The vertebrate rod photoreceptor is divided into three distinct anatomic compartments: the rod OS, which contains hundreds of membrane disks stacked within a plasma membrane envelope; the IS, which contains the biosynthetic machinery, including the mitochondria, the ER, and the Golgi apparatus; and the cell body, which contains the nucleus and the synaptic terminal. The OS and IS are joined by a nonmotile connecting cilium. Photoreceptors contain two populations of microtubules, both of which are organized with uniform polarity (Troutt and Burnside, 1988). Axonemal microtubules nucleate from the basal body at the distal end of the IS and extend in a 9+0 configuration through the connecting cilium into the OS. Singlet cytoplasmic microtubules are longitudinally aligned with their minus ends directed toward the basal bodies and their plus ends toward the synaptic terminal.

(B) Rhodopsin is a seven-transmembrane G protein–coupled receptor with its C terminus facing into the cytoplasm. Four autosomal dominant RP mutations (V345M, P347L, P347S, and Q344ter) found in the C-terminal region of rhodopsin were tested in this report. The Q344ter nonsense mutation lacks the last five amino acids. Also shown is the specific trypsin cleavage site at Lys339 (Hargrave et al., 1982). Two mAbs were used for rhodopsin detection: 1D4 and B6-30 recognize the C-terminal eight residues and the N-terminal residues 3–14, respectively (Molday and MacKenzie, 1983; Adamus et al., 1988).

been previously demonstrated to be a 14 kDa cytoplasmic DLC and also a component of flagellar inner arm dynein I1 (King et al., 1996b; Harrison et al., 1998). Despite its name, Tctex-1 appears to be ubiquitously expressed (Watanabe et al., 1996; King et al., 1996b), and in fibroblasts, it localizes to the Golgi apparatus and microtubules (Tai et al., 1998).

In this report, we demonstrate that rhodopsin's C-terminal cytoplasmic tail interacts with Tctex-1 directly and with high specificity. Rhodopsin-containing membrane vesicles associate with microtubules, both biochemically and functionally, via cytoplasmic dynein in a Tctex-1-dependent manner. We conclude that rhodopsin is an integral membrane cargo receptor for cytoplasmic dynein and that this interaction occurs via the light chain Tctex-1. This represents a novel mode of dynein–cargo interaction in which a DLC directly binds to a cargo molecule receptor located on membrane vesicles. Immunoelectron microscopy of photoreceptors shows that Tctex-1 is associated with rhodopsin-bearing membrane vesicles and is present at the apical membrane

of the IS, supporting the notion that cytoplasmic dynein is involved in the vectorial transport of post-Golgi vesicles bearing rhodopsin in vivo. Finally, several naturally occurring C-terminal rhodopsin mutants have markedly reduced affinities for Tctex-1, which may explain the mistargeting of these mutant rhodopsins in photoreceptors.

Results

Isolation of Tctex-1, a Cytoplasmic Dynein Light Chain, by Interaction with the Carboxy Terminus of Rhodopsin

We searched for proteins that interact with the C terminus of rhodopsin using the yeast two-hybrid system. A bait construct encoding a fusion protein containing a triple repeat of the C-terminal 39 residues of human rhodopsin was used to screen a bovine retinal cDNA library, and a $lacZ^+$, his^+ clone isolated from several independent screenings was chosen for further study. This positive clone grew on histidine-deficient (His⁻) medium (Figure 2A, upper panel) and activated GAL4-dependent $lacZ$ gene expression (data not shown) in the presence of the rhodopsin bait plasmid (pDB-Rho39Tr), but not alone (data not shown) or with three irrelevant control baits (Figure 2A, upper panel). This cDNA clone encoded the bovine ortholog (Tai et al., 1998) of the murine $tctex-1$ (Lader et al., 1989) and human $TCTEL1$ (Watanabe et al., 1996) genes, which encode a 14 kDa cytoplasmic DLC (King et al., 1996b). Bovine and human Tctex-1 proteins are 100% identical at the amino acid level.

In contrast, RP3, another 14 kDa cytoplasmic DLC (Roux et al., 1994; King et al., 1998) that shares 75% amino acid similarity with bovine Tctex-1, did not interact with rhodopsin's C terminus in this system (Figure 2A, lower panel).

To confirm that the Tctex-1-rhodopsin interaction in the yeast two-hybrid system was direct, purified glutathione S-transferase (GST)-Tctex-1 fusion protein was tested for its ability to bind in vitro to a maltose-binding protein (MBP) fusion protein containing a triple repeat of rhodopsin's C-terminal 39 residues (MBP-Rho39Tr). GST-Tctex-1 and bound proteins were eluted from glutathione–Sepharose beads, and MBP-Rho39Tr was detected by immunoblotting with the anti-rhodopsin C terminus mAb 1D4. MBP-Rho39Tr bound specifically to immobilized GST-Tctex-1 (Figure 2B, lane 1) but not to GST alone (Figure 2B, lane 3). Moreover, native rhodopsin in retinal detergent lysates bound to GST-Tctex-1 (Figure 2B, lane 2) but not GST (Figure 2B, lane 4). Similar amounts of GST-Tctex-1 (Figure 2C, lanes 1 and 2) and GST (Figure 2C, lanes 3 and 4) were loaded as confirmed by Coomassie blue staining of a duplicate gel, despite some degradation of GST-Tctex-1 (Figure 2C, lanes 1 and 2).

Naturally Occurring Carboxy-Terminal Rhodopsin Mutations Abolish Tctex-1 Association

Previous reports showing that C-terminal rhodopsin mutants failed to localize efficiently to the rod OS prompted us to determine whether this defect might result from a reduction in affinity for Tctex-1 and hence inefficient
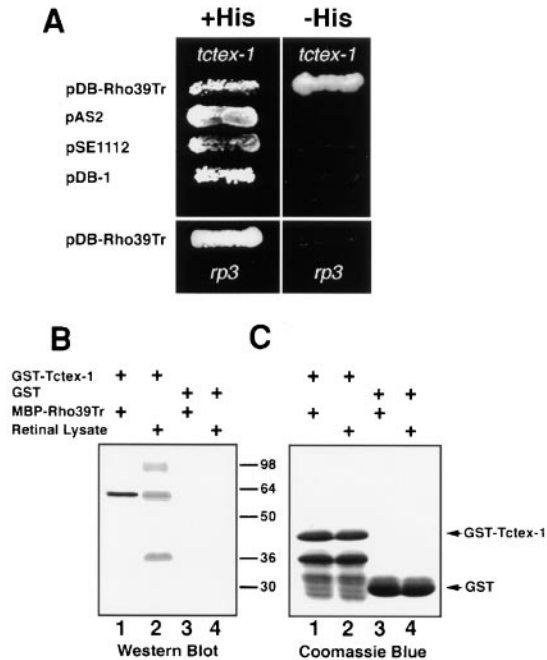
Figure 2. Interaction between Tctex-1 and Rhodopsin's C Terminus in the Yeast Two-Hybrid System and In Vitro

(A) (Upper panel) The *Saccharomyces cerevisiae* yeast strain Y190 containing the two-hybrid isolate *tctex-1* fused to the GAL4-AD was cotransformed with the bait construct pDB-Rho39Tr encoding the rhodopsin C terminus fused to the GAL-DB or with the GAL4-DB alone (pAS2), GAL4-DB fused to the irrelevant yeast SNF1 protein (pSE1112), or GAL4-DB fused to 19 residues (aa135–aa153) of the second cytoplasmic loop of rhodopsin (pDB-1). All double transformants were plated on +His or −His/25 mM 3-aminotriazole synthetic medium. (Lower panel) Yeast transformants cotransformed with RP3 fused to GAL4-AD and with pDB-Rho39Tr were plated on +His and −His media.

(B) Glutathione–Sepharose beads bound to purified GST-Tctex-1 fusion protein (lanes 1 and 2) and GST proteins (lanes 3 and 4) were incubated with bacterial lysates containing MBP fused to a triple repeat of rhodopsin's C terminus (MBP-Rho39Tr; lanes 1 and 3) or with a human retinal detergent lysate (lanes 2 and 4). After washing, proteins eluted with glutathione were separated by SDS-PAGE and immunoblotted with mAb 1D4, which recognizes rhodopsin's C terminus. MBP-Rho39Tr (lane 1) and human rhodopsin (lane 2) bound to GST-Tctex-1 specifically but not to GST alone (lanes 3 and 4). Native rhodopsin (monomer size ∼36 kDa) aggregates to form multimers in SDS sample buffer (Sung et al., 1991b).

(C) Eluates from duplicate binding reactions were separated by SDS-PAGE and stained by Coomassie blue to demonstrate that similar amounts of GST-Tctex-1 (lanes 1 and 2) and GST (lanes 3 and 4) were used for each binding reaction. The low-molecular-weight proteins in the GST-Tctex-1 fusion protein lanes are proteolytic degradation products.

transport by cytoplasmic dynein. Four MBP-Rho39 fusion proteins encoding rhodopsin's C terminus carrying mutations corresponding to those found in patients with autosomal dominant RP—Q344ter, V345M, P347S, and P347L (Figure 1B; Dryja et al., 1990, 1991; Sung et al., 1991a)—were tested for binding to GST-Tctex-1 compared to the wild-type MBP-Rho39 protein. Equal amounts of these MBP-fusion proteins (Figure 3, first panel) were mixed with GST-Tctex-1 or GST. Proteins eluted along with GST-Tctex-1 (Figure 3, second panel) or GST (Figure 3, third panel) from glutathione–Sepharose were
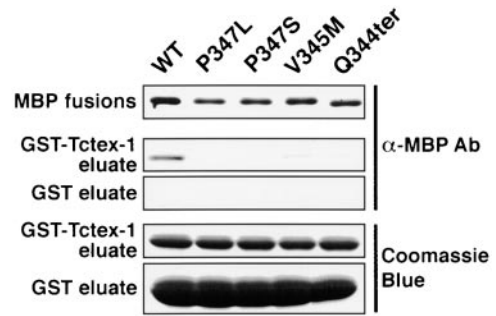
Figure 3. Reduced Binding of Tctex-1 to RP Mutant Rhodopsin C Termini

MBP-Rho39 fusion proteins containing the wild-type rhodopsin sequence (WT) or mutant sequences—P347L, P347S, V345M, or Q344ter—were tested for their ability to bind Tctex-1 in the same system described in Figure 2B. (Panel 1) Similar amounts of each MBP-fusion protein were used in each binding reaction, demonstrated by immunoblotting aliquots of the binding assay mixtures with anti-MBP antibody. (Panels 2 and 3) Proteins coeluting with GST-Tctex-1 (panel 2) or GST (panel 3) from glutathione–Sepharose beads were separated on SDS-PAGE and immunoblotted with anti-MBP antibody. (Panels 4 and 5) Duplicate gels were stained with Coomassie blue to demonstrate that similar amounts of GST-Tctex-1 (panel 4) and GST (panel 5) were used for each binding reaction.

immunoblotted with anti-MBP antibody (Figure 3, second and third panels). Little or none of each of the mutant MBP-fusion proteins could be coeluted with GST-Tctex-1 relative to the wild-type control (Figure 3, second panel), indicating that the binding affinities of all four mutant MBP-Rho39 fusions to Tctex-1 were significantly reduced compared to the wild-type rhodopsin sequence. No degradation of any of the MBP-fusion proteins could be detected (Figure 3, first panel), and the amounts of GST-Tctex-1 and GST eluted from each binding reaction were similar, based on Coomassie blue staining (Figure 3, fourth and fifth panels, respectively). The observed inhibition of Tctex-1 binding by these mutations is likely to be specifically sequence dependent and not the result of an overall conformational alteration of this region, as C-terminal mutant rhodopsins do not show significant defects in C-terminal-dependent phototransduction functions in vitro and in vivo (Sung et al., 1994; Weiss et al., 1995).

Rhodopsin-Bearing Vesicles Cosediment with Microtubules in the Presence of Cytoplasmic Dynein in a Tctex-1-Dependent Manner

We tested the nature of the interaction between rhodopsin-bearing vesicles and cytoplasmic dynein complexes by using a microtubule cosedimentation assay. These vesicles, prepared by sonicating purified bovine rod OS, are similar to rhodopsin-bearing post-Golgi vesicles in terms of their high surface density of rhodopsin and overall protein composition (Deretic and Papermaster, 1991). Rhodopsin was by far the most abundant protein on these vesicles, as can be seen by Coomassie blue staining (Figure 4A, lanes 2 and 3) and immunoblotting (Figure 4A, lane 4), consistent with reports that rhodopsin makes up about 95% of OS disk membrane protein
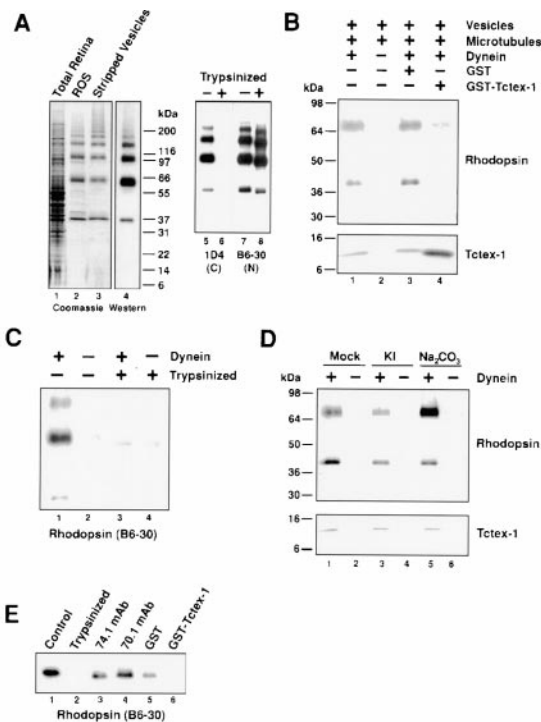
Figure 4. Cosedimentation of Rhodopsin-Bearing Vesicles with Microtubules in a Cytoplasmic Dynein-, Tctex-1-, and Rhodopsin C Terminus–Dependent Manner

(A) Composition and topology of rhodopsin-bearing vesicles. A total retina detergent extract (lane 1), purified ROS (lanes 2 and 4), and Na₂CO₃ (pH 11.5) stripped sonicated ROS vesicles (lane 3) were separated by SDS-PAGE and stained by Coomassie blue (lanes 1–3) or immunoblotted for rhodopsin (lane 4). Trypsinized (lanes 6 and 8) or mock-trypsinized (lanes 5 and 7) vesicles were separated on SDS-PAGE and immunoblotted using mAb 1D4 (lanes 5 and 6) or B6-30 (lanes 7 and 8). Note the small shift in rhodopsin mobility (lane 8) and loss of 1D4 reactivity (lane 6) upon trypsinization, indicative of specific cleavage of the C-terminal nine residues at Lys-339 (Hargrave et al., 1982).
(B) Rhodopsin-bearing vesicles were incubated in the presence (lanes 1, 3, and 4) or absence (lane 2) of purified cytoplasmic dynein, mixed with Taxol-stabilized microtubules assembled from purified tubulin, and centrifuged through a sucrose cushion to sediment microtubules with bound dynein and vesicles. A 100-fold molar excess of GST (lane 3) or GST-Tctex-1 (lane 4) relative to dynein was used in competition assays. The pellet was separated on SDS-PAGE and immunoblotted for rhodopsin (upper panel) or Tctex-1 (lower panel). The greater amount of Tctex-1 in lane 4 is due to proteolytic release of Tctex-1 from GST-Tctex-1 fusion protein.
(C) Cosedimentation assay performed with trypsinized (lanes 3 and 4) or mock-trypsinized (lanes 1 and 2) rhodopsin-bearing vesicles in the presence (lanes 1 and 3) or absence (lanes 2 and 4) of purified cytoplasmic dynein.
(D) Cosedimentation assay performed with untreated (lanes 1 and 2), 0.6 M KI-stripped (lanes 3 and 4), or 0.1 M Na₂CO₃ (pH 11.5) stripped (lanes 5 and 6) rhodopsin-bearing vesicles in the presence (lanes 1, 3, and 5) or absence (lanes 2, 4, and 6) of purified cytoplasmic dynein.
(E) Crude rat brain cytosol can also support cosedimentation of rhodopsin-bearing vesicles with microtubules. Vesicles (lanes 1 and 3-6) or trypsinized vesicles (lane 2) were incubated with brain cytosol, treated with Taxol to polymerize microtubules from endogenous tubulin, and centrifuged over a sucrose cushion. mAbs 74.1 (lane 3) or 70.1 (lane 4) against DIC and GST (lane 5) or GST-Tctex-1 (lane 6) were added to brain cytosol before performing the cosedimentation assay.

(Krebs and Kühn, 1977). As previously reported (Hargrave et al., 1982), trypsinization of these vesicles nearly completely removed reactivity to the C terminus–specific 1D4 mAb (Figure 4A, lane 6; see legend). In contrast, the luminal N-terminal epitope recognized by the B6-30 mAb was protected from proteolysis (Figure 4A, lane 8), indicating that the sonicated vesicles remained right-side out.

In the cosedimentation assay, rhodopsin-bearing vesicles preincubated with purified rat brain cytoplasmic dynein were briefly incubated with Taxol-stabilized microtubules assembled from purified tubulin. The microtubules and associated materials were then pelleted by centrifugation through a sucrose cushion to separate them from unbound vesicles, which floated at the interface. The presence of rhodopsin in the resulting microtubule pellet was analyzed by SDS-PAGE and immunoblotting.

We found that rhodopsin-bearing vesicles cosedimented with microtubules in the presence of cytoplasmic dynein (Figure 4B, lane 1). In contrast, rhodopsin was not detected in the microtubule pellet when dynein was omitted (Figure 4B, lane 2), indicating that rhodopsin-bearing vesicle cosedimentation with microtubules occurs through interaction with the cytoplasmic dynein complex. Addition of excess GST-Tctex-1, but not GST, was able to abolish vesicle cosedimentation with microtubules even in the presence of cytoplasmic dynein (Figure 4B, lanes 3 and 4). This result strongly argues that rhodopsin associates with cytoplasmic dynein via Tctex-1.

On the other hand, we found that treatment of vesicles with trypsin prevented them from cosedimenting with microtubules in the presence of dynein (Figure 4C, lane 3). This result indicates that the reported ability of cytoplasmic dynein to interact with phospholipid vesicles in vitro (Lacey and Haimo, 1994; Muresan et al., 1996) cannot account for the observed behavior of rhodopsin-bearing vesicles in this system.

To be certain that peripheral membrane proteins on rhodopsin-bearing vesicles were not required for association with cytoplasmic dynein, vesicles stripped with either KI or alkali (Na₂CO₃) were used in the microtubule cosedimentation assay. KI-stripped (Figure 4D, lane 3) and alkali-stripped vesicles (Figure 4D, lane 5; see Figure 4A, lane 3 for protein composition) remained competent, like untreated vesicles (Figure 4D, lane 1), to bind to microtubules in a dynein-dependent manner (Figure 4D, lanes 2, 4, and 6).

We also performed the microtubule cosedimentation assay using crude rat brain cytosolic extract. Rhodopsin-bearing vesicles cosedimented with microtubules polymerized from endogenous tubulin present in brain cytosol (Figure 4E, lane 1) in a Tctex-1-dependent manner (Figure 4E, lane 6). This cosedimentation was blocked by pretrypsinization of the vesicles (Figure 4E, lane 2). Note that only 50 ng of rhodopsin was used in these cosedimentation assays, corresponding to concentrations of ∼10–50 nM. We therefore conclude that the affinity of cytoplasmic dynein/Tctex-1 for rhodopsin is sufficiently high that a stable and specific interaction can form in a physiologically complex and relevant mixture of proteins.

Finally, we tested the possible role of dynactin in the

interaction of cytoplasmic dynein with rhodopsin-bearing vesicles. Dynactin is also present in sucrose gradient–purified dynein and has been postulated to mediate the binding of dynein to at least some of its cargoes (Vallee et al., 1995). We used the anti-DIC mAbs 70.1 (Steuer et al., 1990) and 74.1 (Dillman and Pfister, 1994), which recognize the N terminus of DIC and block its ability to interact with the p150^{Glued} dynactin subunit (Steffen et al., 1997). Rat brain cytosol was preincubated with the antibodies at a final concentration of 0.2 mg/ml, which is 2-fold higher than the concentration demonstrated to be effective in blocking dynein–dynactin interaction (Steffen et al., 1997). These antibodies did not abolish rhodopsin-bearing vesicle cosedimentation with microtubules in brain cytosol (Figure 4E, lanes 3 and 4) or using purified cytoplasmic dynein (data not shown). This result suggests that the dynein–dynactin interaction is not strictly required for stable dynein/Tctex-1 binding to rhodopsin-bearing vesicles.

Cytoplasmic Dynein Translocates Rhodopsin-Bearing Vesicles on Microtubules

Our binding assays provided evidence that rhodopsin is likely to act as a cytoplasmic dynein receptor via an interaction with Tctex-1, and we therefore adapted existing microtubule-based motility assays to examine whether rhodopsin-bearing vesicles could be translocated by cytoplasmic dynein along immobilized microtubules. In this assay, vesicles were fluorescently labeled with DiI-C$_{18}$, a carbocyanine dye that readily incorporates into lipid bilayers. Immunofluorescent labeling of the DiI-labeled vesicles with an anti-rhodopsin monoclonal antibody revealed that 97.2% $\pm$ 0.7% of the DiI-labeled vesicles contained detectable rhodopsin (data not shown). The fluorescent vesicles were first allowed to bind freshly purified rat brain cytoplasmic dynein. Taxol-stabilized rhodamine-labeled microtubules were prepared and attached to the surface of a glass coverslip mounted in a perfusion chamber. Finally, the fluorescent vesicles bound to dynein were introduced into the chamber in the presence of ATP, and movements were recorded by time-lapse imaging.

In the presence of dynein, vesicles were observed to bind to microtubules, and a fraction of these displayed unidirectional motility along the microtubules. Examples of unidirectional movement of vesicles along microtubules can be seen in Figures 5A and 5B. The mean velocity of these movements was 0.76 $\pm$ 0.1 μm/s (n = 8), well within the range of 0.2–1.2 μm/s and mean of 0.6 μm/s previously reported for sucrose gradient–purified cytoplasmic dynein (Schroer and Sheetz, 1991). In the absence of dynein or in the presence of excess GST-Tctex-1, little or no vesicle attachment to microtubules was observed, and no movements were seen (data not shown).

We tested whether rhodopsin's C terminus was specifically required for the interaction of DiI-labeled rhodopsin-bearing vesicles with cytoplasmic dynein and fluorescent microtubules by preincubating vesicles with either 1D4 or B6-30 Fab and counting the number of vesicles bound to microtubules. As can be seen in Figure 5C, we found that the mean number of bound vesicles per unit length of microtubule was significantly (p < 0.05)
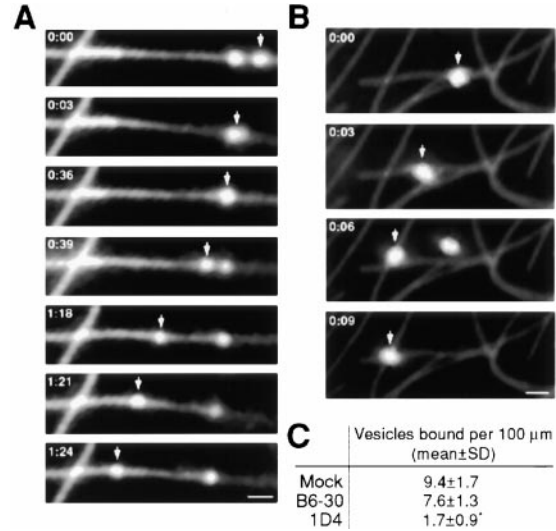
Figure 5. Unidirectional Translocation of Rhodopsin-Bearing Vesicles on Microtubules by Cytoplasmic Dynein

(A and B) Several frames are shown from two examples of dynein-based vesicle motility. Arrows indicate the positions of moving vesicles. Fluorescent microtubules polymerized from rhodamine-conjugated and unlabeled tubulin (1:5 ratio) were immobilized in a perfusion chamber with anti-tubulin antibody. Fluorescent rhodopsin-bearing vesicles labeled with DiI were incubated with cytoplasmic dynein, diluted into motility buffer containing ATP, and introduced into the perfusion chamber. Vesicle motility was recorded by time-lapse imaging. Bars, 2 μm.

(C) Table summarizing the effects of anti-rhodopsin Fab fragments on vesicle–microtubule binding. Fluorescent rhodopsin-bearing vesicles were preincubated in the absence or presence of either 1D4 or B6-30 Fab and then incubated with cytoplasmic dynein and added to fluorescent microtubules. For each experimental condition, the means and standard deviations of the number of vesicles bound per 100 μm of microtubule in three independent trials are shown. *, p < 0.05 for 1D4 treatment relative to either B6-30 or mock treatment.

decreased by 1D4 Fab compared to mock treatment or treatment with B6-30 Fab. No significant effect by B6-30 Fab relative to mock treatment was observed. We therefore conclude that the distal C terminus of rhodopsin is essential for rhodopsin-bearing vesicles to interact with the cytoplasmic dynein complex.

Tctex-1 Is Present in Photoreceptor Inner Segments

To confirm that Tctex-1 was in fact present in rod photoreceptor IS, where the post-Golgi trafficking of rhodopsin occurs, we performed immunocytochemical analysis of retinal sections using an affinity-purified anti-Tctex-1 antibody. The specificity of this antibody has been previously demonstrated; it recognizes a single band on immunoblots of retinal lysates from rats and several other species and does not recognize the closely related DLC RP3 (Tai et al., 1998). In mouse photoreceptors, strikingly punctate Tctex-1 immunoreactivity was detected in the IS (Figures 6A and 6B), suggesting that a significant fraction of Tctex-1 is membrane associated in photoreceptors. Furthermore, more intense Tctex-1 immunoreactivity was found in the Golgi-enriched proximal IS (Figure 6B, arrowhead), consistent with its Golgi
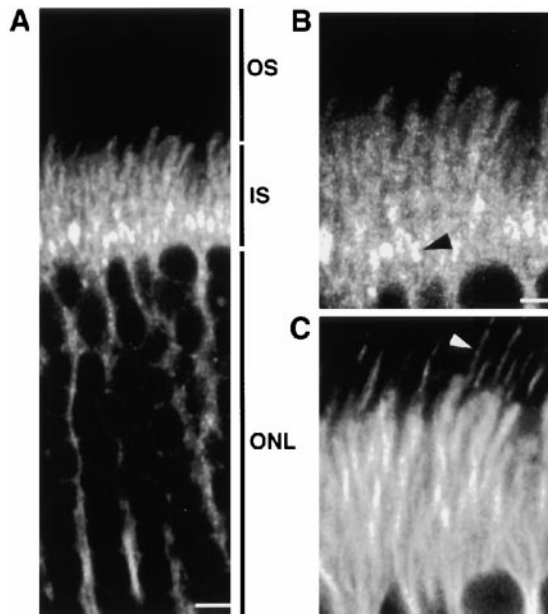
Figure 6. Tctex-1 in the Inner Segments of Mouse Photoreceptors

(A) Immunofluorescent localization of Tctex-1 in a 1 μm confocal microscope section of mouse outer retina. The outer retina contains the photoreceptor nuclei in the outer nuclear layer (ONL), photoreceptor IS, and photoreceptor OS. Bar, 5 μm.

(B and C) Enlarged region showing detail of Tctex-1 staining (B) in IS double labeled for α-tubulin (C). The black arrowhead in (B) indicates the Golgi-enriched proximal inner segment. Note the presence of tubulin, but not Tctex-1, in the connecting cilium (white arrowhead in [C]). Bar, 2 μm.

localization in fibroblasts (Tai et al., 1998). Tctex-1 immunoreactivity was not detected in connecting cilia, which were visualized by double labeling with anti-α-tubulin antibody (Figure 6C, arrowhead). Very little or no Tctex-1 immunoreactivity could be detected in the OS of photoreceptors. Tctex-1 immunostaining was also observed in other layers of the retina, most notably at synapses in the plexiform layers and along nerve fibers (data not shown). Immunofluorescent double labeling of retinal sections for dynein heavy chain and Tctex-1 revealed virtually complete colocalization within the IS at the level of confocal microscopy (data not shown).

Tctex-1 Colocalizes with Rhodopsin in Photoreceptor Inner Segments

In ultrathin sections of mouse retina, immunoelectron microscopy of the apical domains of IS revealed abundant Tctex-1 labeling near the apical plasma membrane, especially at the base of the connecting cilium (Figure 7A, arrowheads), which are both sites of delivery for IS rhodopsin transport vesicles (Deretic and Papermaster, 1991; Besharse and Wetzel, 1995). Despite the use of highly sensitive silver-enhanced immunogold labeling, no Tctex-1 reactivity above background was seen in the photoreceptor OS or in the connecting cilium itself (Figure 7A).

Double labeling of Tctex-1 and rhodopsin revealed striking colocalization of the two proteins in the IS of rod photoreceptors (Figures 7B and 7C, arrowheads). This finding is evidence that cytoplasmic dynein/Tctex-1

interacts with rhodopsin in vivo and provides the molecular basis to explain the known vectorial transport of rhodopsin to the OS.

Discussion

Tctex-1 Is a Cargo-Binding Subunit of Cytoplasmic Dynein, and Rhodopsin Is a Dynein "Receptor"

Cytoplasmic dynein has been implicated in the movement of a diverse array of cargoes ranging from kinetochores (Steuer et al., 1990) to Golgi membranes (Corthésy-Theulaz et al., 1992). Previous studies have suggested that the association of dynein with its cargoes is nonspecific, since cytoplasmic dynein can bind to pure phospholipid liposomes (Lacey and Haimo, 1994; Muresan et al., 1996). However, the ability of cytoplasmic dynein to mediate a wide range of activities suggests that it may have specific docking mechanisms for specific types of cargo. Our present results reveal that rhodopsin not only directly interacts with Tctex-1 but also functionally associates with cytoplasmic dynein and its motor activity. Furthermore, we find that the interaction of cytoplasmic dynein with its cargo can be quite specific. We propose, therefore, that the interaction between rhodopsin and Tctex-1 represents a novel mode of dynein–cargo interaction in which a dynein subunit directly binds to an integral membrane protein cargo molecule that serves as a dynein receptor.

Given that rhodopsin acts as an integral membrane protein receptor for dynein, then Tctex-1 appears to be a cargo-binding subunit of cytoplasmic dynein. The ubiquitous expression of Tctex-1 suggests that it may bind to additional cytoplasmic dynein cargo molecules or receptors other than rhodopsin. Indeed, it has been recently reported that Tctex-1 interacts with several other proteins: pp59[fyn] (Campbell et al., 1998; Mou et al., 1998), CD5 (Bauch et al., 1998), and Doc2 (Nagano et al., 1998). This is also consistent with our previous results showing that a substantial fraction of Tctex-1 localizes to the Golgi apparatus in fibroblasts (Tai et al., 1998), which suggests there may be additional target(s) of Tctex-1 binding on or near the Golgi apparatus. Thus, this novel mode of dynein–cargo interaction via a DLC may be a general phenomenon.

Tctex-1 is unlikely to be the sole cytoplasmic dynein cargo-binding subunit. The great diversity of known cytoplasmic dynein cargoes and functions implies not only the existence of multiple dynein receptors but also the existence of multiple cargo-binding dynein subunits (or isoforms). A favored model for dynein–cargo binding has been the interaction between the DIC and the dynactin complex via the p150[Glued] dynactin subunit (Vaughan and Vallee, 1995). The dynactin complex has been shown to be involved in many of the same processes as cytoplasmic dynein and has been postulated to anchor dynein to its cargoes (Plamann et al., 1994; McGrail et al., 1995; Echeverri et al., 1996). Although we found that the dynein–dynactin interaction is not absolutely necessary for dynein to bind stably to rhodopsin-bearing vesicles, it must be stressed that this result does not exclude a role for dynactin in promoting vesicle motility or in strengthening dynein–vesicle or dynein–microtubule interaction. It is conceivable that the binding of cytoplasmic dynein to any given cargo organelle or vesicle
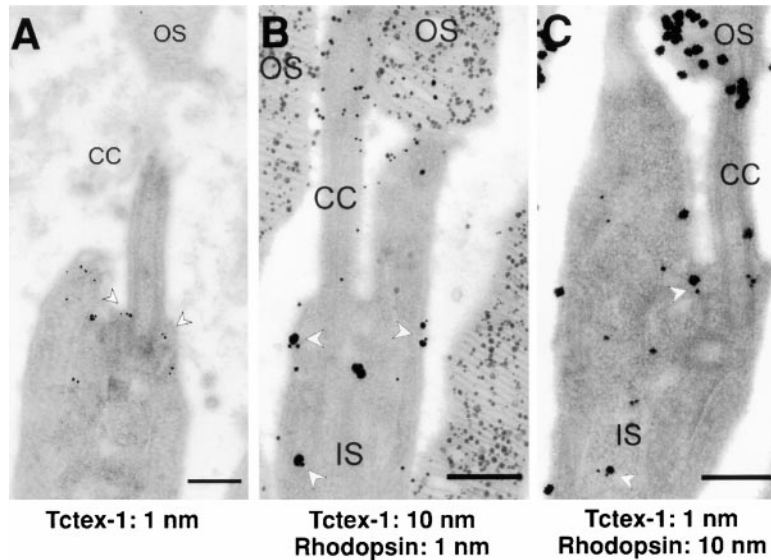
Figure 7. Tctex-1 Colocalization with Rhodopsin within the Inner Segment

(A) Immunoelectron microscopy of silver-enhanced immunogold Tctex-1 labeling in ultrathin sections of mouse retina. View of the apical IS connecting cilium (CC) and OS of rod photoreceptor, showing abundant Tctex-1 labeling near the apical IS plasma membrane as well as at the base of the connecting cilium (arrowheads).

(B and C) Double-label silver-enhanced immunogold labeling for Tctex-1 and rhodopsin in mouse rod photoreceptors. Arrowheads indicate examples of Tctex-1 and rhodopsin colocalization in the apical IS. (B) Tctex-1 and rhodopsin labeled with 10 nm and 1 nm gold particles, respectively. (C) Tctex-1 and rhodopsin labeled with 1 nm and 10 nm gold particles, respectively. Bars, 250 nm.

involves more than one dynein or dynactin subunit (and conversely, more than one receptor on the cargo), which would add the advantage of greater specificity.

The identification of multiple DIC isoforms (Vaughan and Vallee, 1995), some of which are tissue specific (Pfister et al., 1996), has prompted speculation that they mediate binding to different cargoes. Tctex-1 itself has five known relatives (King et al., 1996b), at least one of which, RP3, is also a DLC (King et al., 1998) but does not bind to the C terminus of rhodopsin. This raises the interesting possibility that Tctex-1-related DLCs also mediate binding to as yet unidentified dynein receptors distinct from those that bind to Tctex-1.

The known diversity of dynein subunit isoforms, as well as our finding (Tai et al., 1998) that dynein subunits may not all be assembled into complexes at steady state, implies that there must be heterogeneity in the composition of dynein complexes. Understanding this heterogeneity and its regulation may be important for understanding how dynein is able to mediate a wide range of specific transport functions.

Microtubule-Based Transport and the Vectorial Targeting of Rhodopsin in Photoreceptors

The photoreceptor OS is continually being turned over, as each day new membrane disks containing rhodopsin are produced at the base of the OS and old disks are shed from the distal end of the OS (Young, 1976). Due to this rapid OS turnover, rhodopsin, which comprises ~95% of total OS disk membrane protein, must be continually synthesized and transported to the OS. Despite the resulting large flux of rhodopsin through the IS, little rhodopsin can be found on the plasma membrane of the IS and cell body, in contrast to the extremely high density of rhodopsin found in OS membranes. Thus, photoreceptors must have an efficient, and probably active, transport mechanism.

In the IS, the minus ends of microtubules are oriented toward the base of the photoreceptor OS. Given our evidence that cytoplasmic dynein directly and functionally associates with rhodopsin via Tctex-1, we propose that cytoplasmic dynein mediates the vectorial translocation of rhodopsin-bearing post-Golgi vesicles along microtubules in the rod IS. This is also supported by the colocalization of Tctex-1 and rhodopsin in the photoreceptor IS. The ability of cone opsins to directly interact with cytoplasmic dynein was not tested.

The lack of significant Tctex-1 labeling in the photoreceptor OS and the accumulation of Tctex-1 at the base of the connecting cilium as seen by immunoelectron microscopy suggest that the interaction between cytoplasmic dynein and rhodopsin-bearing vesicles is regulated. We hypothesize that rhodopsin is released from dynein/Tctex-1, perhaps by dynein posttranslational modification, prior to its passage through the connecting cilium. Soluble Tctex-1/dynein is prevented from reaching the OS, since the polarity of axonemal microtubules in the connecting cilium is reversely oriented (Figure 1A) and/or because the connecting cilium appears to be a diffusion barrier (Spencer et al., 1988). Moreover, although Tctex-1 has been identified as a flagellar inner dynein arm component (Harrison et al., 1998), the photoreceptor connecting cilium is nonmotile and lacks morphologically identifiable dynein arms on electron microscopy (Rohlich, 1975). Thus, it seems that Tctex-1 functions in photoreceptors exclusively as a subunit of cytoplasmic dynein, not flagellar dynein.

How rhodopsin at the apical IS is subsequently incorporated into nascent membrane disks in the OS remains an open question. Two models have been proposed for this transport step from the IS to the OS: a ciliary pathway and an extracellular pathway (Besharse and Wetzel, 1995). Recent immunoelectron microscopic detection of rhodopsin in the ciliary membrane (U. W. and A. Schmitt, unpublished results) supports the ciliary transport model. The role of motor proteins in rhodopsin transport in the connecting cilium is not clear. One set of candidates is the kinesin superfamily proteins, which have been immunohistochemically detected in fish photoreceptors in the area surrounding the basal body and the connecting cilium (Beech et al., 1996). Another is myosin VIIa, which has been localized to the membrane of the mammalian photoreceptor connecting cilium (Liu et al., 1997).

It is conceivable that at the base of the connecting cilium, the rhodopsin cargo is handed over from cytoplasmic dynein to one of these ciliary motor proteins for its final passage through the connecting cilium to the OS.

Rhodopsin Transport in Human Disease

Fourteen naturally occurring mutations have been identified at rhodopsin's distal C terminus in RP patients. Interestingly, the phototransduction functions of the C-terminal mutants tested to date are normal both in vitro and in vivo. The reduced affinity of four of these C-terminal rhodopsin mutants for Tctex-1, and therefore for cytoplasmic dynein, is strikingly consistent with the mislocalization of these mutants in vivo and provides a molecular explanation for the defective transport of these mutants to the rod OS. This is further supported by the ability of a mAb recognizing rhodopsin's C-terminal eight residues as well as specific trypsin cleavage of the C-terminal nine residues to abolish vesicle–dynein interaction. Given that rhodopsin mislocalization is the primary cause of photoreceptor cell death for these mutations, genes required for proper rhodopsin localization should therefore be considered candidates for hereditary retinal degenerations. In fact, *TCTEL1*, the human ortholog of *tctex-1*, has been proposed as a candidate gene for retinal cone dystrophy 1 on the basis of its colocalization to 6q25.2-q25.3 (Watanabe et al., 1996). Further investigation is needed to understand why and how rhodopsin mislocalization triggers photoreceptor degeneration and programmed cell death (Chang et al., 1993; Portera-Cailliau et al., 1994).

Experimental Procedures

Retinal cDNA Library Construction and Two-Hybrid Screening
A bait plasmid (pDB-Rho39Tr) was generated by fusing a triple repeat of the last 39 amino acids (aa310–aa348) of human rhodopsin to the GAL4 DNA-binding domain (GAL4-DB) in the pAS2 vector (Chuang and Sung, 1998). A bovine retinal two-hybrid cDNA library constructed using oligo-dT primed, bovine retinal cDNAs directionally inserted downstream of the GAL4 transcriptional activation domain (GAL4-AD) was transformed into yeast strain Y190 containing the pDB-Rho39Tr bait. Colonies that grew on His⁻/25 mM 3-aminotriazole medium were assayed for β-galactosidase activity by a filter assay (Breeden and Nasmyth, 1985). Plasmids isolated from primary positives were retransformed into Y190 yeast in conjunction with either pDB-Rho39Tr or a number of control baits consisting of irrelevant sequences fused to the GAL4-DB and tested for growth on His⁻ medium and β-galactosidase activity.

Constructs and Bacterial Fusion Protein Production
The MBP-Rho39Tr construct was previously described (Chuang and Sung, 1998). MBP-Rho39 variants containing RP mutations (P347L, P347S, V345M, and Q344ter) were constructed from a series of rhodopsin cDNAs bearing the corresponding amino acid changes (Sung et al., 1991a, 1993). The control bait pDB-1 was generated by inserting a PCR fragment encoding the second cytoplasmic loop of rhodopsin (aa135–aa153) into the pAS2 vector. The full-length *rp3* sequence was PCR amplified from a human retinal cDNA library and inserted into pACTII to generate GAL-AD-RP3. The sequences of all DNA inserts generated from PCR reactions were confirmed by sequencing. The constructs expressing GST-Tctex-1 and MBP-Tctex-1 and the production of the corresponding fusion proteins were previously described (Tai et al., 1998).

In Vitro Fusion Protein Binding Assay
Bacterial pellets containing MBP-Rho39 fusion proteins were resuspended in PBS plus 1% Triton X-100, 1 mg/ml lysozyme, and protease inhibitors (1 mM PMSF, 2 μg/ml aprotinin, 2 μg/ml leupeptin, and 0.7 μg/ml pepstatin). After sonication and centrifugation (18 krpm, 10 min), the supernatants were collected for the binding assay. Retinal lysate was prepared by shearing two human retinas in 800 μl lysis buffer (10 mM Tris-Cl [pH 8.0], 0.3 M NaCl, 2% NP-40, and protease inhibitors) and sonicating for 1 min. The supernatant, after centrifugation, was used for the binding assay. Bacterial or retinal lysate was incubated overnight at 4°C with GST-Tctex-1- or GST-conjugated glutathione–Sepharose (Amersham Pharmacia Biotech, Piscataway, NJ) in binding buffer (20 mM Tris-Cl [pH 7.5], 50 mM KCl, 100 mM NaCl, 2 mM CaCl₂, 2 mM MgCl₂, 5 mM dithiothreitol, and protease inhibitors) supplemented with 1% bovine serum albumin (BSA). After incubation, the beads were washed three times with binding buffer/1% BSA, twice with binding buffer/0.02% Tween-20, and eluted with 60 μl 5 mM glutathione in 50 mM Tris-Cl (pH 8.0). Eluted samples were subjected to SDS-PAGE followed either by staining with Coomassie blue or immunoblotting.

Rhodopsin-Bearing Vesicle Preparation
Rod OS (0.5 mg/ml total protein) isolated from frozen bovine retinas (Smith et al., 1975) were sonicated for 1 min at 50% power in an ice-water slurry in a cup horn driven by a Branson Sonifier 250 (Danbury, CT) to produce rhodopsin-bearing vesicles. The vesicles were pelleted (20 min at 100,000 × g) and resuspended at 50 μg/ml total protein in PEM buffer (80 mM PIPES [pH 6.8], 1 mM EGTA, and 1 mM MgSO₄) followed by brief resonication. In some experiments, vesicles were stripped by incubation in either 0.6 M KI or 0.1 M Na₂CO₃ (pH 11.5) on ice for 15 min. The vesicles were then washed by two cycles of pelleting and resuspension in PEM followed by resonication. For trypsinization experiments, rhodopsin-bearing vesicles (25 μg total protein in 200 μl PEM) were treated with 0.1 mg/ml trypsin for 30 min at 37°C, and the digestion was stopped by adding soybean trypsin inhibitor (1 mg/ml; Sigma). The trypsinized vesicles were then washed by two cycles of pelleting, resuspended in PEM plus 0.5 mg/ml soybean trypsin inhibitor, and briefly resonicated.

Microtubule Cosedimentation Assay
Rat brain cytoplasmic dynein was purified and fractionated by sucrose density gradient centrifugation exactly as described in Collins and Vallee (1989). The purity of the cytoplasmic dynein preparation was confirmed by SDS-PAGE/Coomassie blue staining of sucrose gradient fractions. The activity of each fresh dynein preparation was checked by a microtubule gliding assay (Paschal et al., 1987; Hyman, 1991). Dynein absorbed to a coverslip bound microtubules at high density, and all of these microtubules were seen to move continuously and unidirectionally at rates of ∼0.5–1.2 μm/s upon addition of ATP.

Tubulin was also purified from rat brain and polymerized into microtubules (Collins and Vallee, 1987). Microtubule-associated proteins were removed during purification prior to microtubule disassembly by incubation with 0.5 M NaCl for 10 min at room temperature (RT) followed by centrifugation to sediment the microtubules. The purified tubulin was at least 95% pure on SDS-PAGE/Coomassie blue staining.

For the cosedimentation assay, rhodopsin-bearing vesicles (50 ng total protein) in PEM were first incubated with 0.5 μg of purified cytoplasmic dynein at RT for 1 hr. For competition experiments, 1.9 μg of purified GST-Tctex-1 or 1.3 μg of GST (100-fold molar excess over dynein) was also included. The vesicle–dynein mixture was then added to 25 μg of Taxol-stabilized microtubules for an additional 10 min at 30°C. Finally, the microtubule-vesicle-dynein mixture was layered over a cushion of 1 M sucrose in PEM/Taxol buffer and centrifuged in a TLS55 rotor (Beckman, Palo Alto, CA) at 40,000 × g for 30 min at 30°C. The pellet was resuspended in SDS sample buffer, separated by SDS-PAGE, and immunoblotted with the anti-rhodopsin mAb B6-30 and Tctex-1 antibody (Tai et al., 1998).

Rat brain cytosolic extract was prepared as described in protocols for cytoplasmic dynein purification (Collins and Vallee, 1989). For

cosedimentation experiments, rhodopsin-bearing vesicles were incubated with brain cytosol for 30 min at RT; microtubules were polymerized with 20 μM Taxol and then pelleted through a sucrose cushion as described above. For dynein–dynactin blocking experiments, brain cytosol was preincubated with mAbs against DIC-74.1 (Chemicon International, Temecula, CA) or 70.1 (Sigma) at a final concentration of 0.2 mg/ml for 1 hr on ice before the addition of vesicles. For competition experiments, GST and GST-Tctex-1 were used at a final concentration of 0.1 mg/ml.

Rhodopsin-Bearing Vesicle Motility Assay

Existing motility assays (Hyman, 1991; Wang et al., 1995) were adapted as follows. Rhodopsin-bearing vesicles (20 μg total protein) were fluorescently labeled by incubation in 5 μM DiI-C$_{18}$ (Molecular Probes, Eugene, OR) in PEM buffer on ice for 10 min. Labeled vesicles were collected and washed three times by pelleting and resuspending in PEM and then resonicated. Rhodamine-labeled microtubules were polymerized with an average length of 10 μm from rhodamine–tubulin and unlabeled tubulin (Cytoskeleton, Denver, CO) at a ratio of 1:5 according to the supplier's instructions. Perfusion chambers were prepared by attaching acid-washed 22 mm $\times$ 22 mm no. 1 coverslips to acid-washed slides using 3M double-sided tape.

Fluorescent vesicles were then incubated with freshly purified rat brain cytoplasmic dynein for 1 hr on ice. Fluorescent microtubules were immobilized on the surfaces of the perfusion chamber and blocked with 5 mg/ml α-casein in PEM with 20 μM Taxol. At this point, the fluorescent vesicle–dynein mixture was diluted 1:20 into low ionic strength motility buffer (10 mM PIPES [pH 6.8], 1 mM EGTA, 2 mM MgCl$_2$, 0.2 mM EDTA, 5 mM ATP, and 20 μM Taxol) containing 0.1 mg/ml catalase, 0.05 mg/ml glucose oxidase, 10 mM glucose, 0.3% β-mercaptoethanol, and 4 mM ascorbic acid and then immediately added to the perfusion chamber. Time-lapse images of vesicle motility were recorded by a cooled CCD camera (Princeton Instruments) on a Nikon Eclipse E600 microscope with filters for DiI emission. The system was controlled by MetaMorph software (Universal Imaging, Media, PA).

For antibody blocking experiments, 40 ng of DiI-labeled vesicles was preincubated for 30 min at RT in the absence or presence of 0.8 mg/ml 1D4 or B6-30 Fab prepared using an ImmunoPure IgG1 Fab kit (Pierce, Rockford, IL). These vesicles were then incubated with 60 μg/ml dynein for 30 min. The vesicle–dynein mixture was then added to Taxol-stabilized fluorescent microtubules, incubated for 5 min at RT, and added to a perfusion chamber. Twenty-five random fields were imaged by fluorescence microscopy for each experimental condition, and the number of vesicles bound per 100 μm of microtubule was determined.

Immunohistochemistry of Mouse Retina

Eyecups prepared from C57BL6/J mice were fixed in 4% paraformaldehyde and 0.08% glutaraldehyde in 0.1 M cacodylate buffer (pH 7.2) at 4°C for 3 hr. Small pieces of eyecup were then embedded in 5% SeePlaque low-melt agarose (FMC, Rockland, ME) in PBS-C/M (PBS plus 0.2 mM CaCl$_2$ and 2 mM MgCl$_2$). Forty micrometer sections were cut on a Vibratome (Technical Products International, St. Louis, MO) in ice-cold PBS-C/M and then quenched in 50 mM NH$_4$Cl in PBS-C/M for 10 min. The sections were blocked in 5% normal goat serum in PBS-C/M for 30 min and incubated with anti-Tctex-1 antibody (1 μg/ml) and anti-α-tubulin mAb (Amersham Pharmacia Biotech; 1:1000) in blocking solution/0.1% Triton X-100 overnight at 4°C. The sections were then rinsed in PBS-C/M and incubated in Alexa-conjugated secondary antibodies (diluted 1:200 in PBS-C/M; Molecular Probes) for 2 hr. Sections were examined by confocal microscopy (Molecular Dynamics, Sunnyvale, CA).

Immunoelectron Microscopy

Eyecups prepared from C57BL6/J mice were fixed in 0.1% glutaraldehyde and 4% paraformaldehyde in 0.1 M phosphate buffer (pH 7.4) for 3 hr at RT. Small pieces of fixed eyecup were dehydrated to 98% ethanol, embedded in LR White, and polymerized at 4°C under indirect UV light.

Ultrathin sections (60–70 nm) were collected on formvar-coated nickel grids. Some sections were first etched with saturated sodium periodate at RT for 3 min. The grids were preincubated with 0.1% Tween 20 in PBS, quenched with 50 mM NH$_4$Cl in PBS, and incubated in blocking buffer (0.1% ovalbumin and 0.5% cold water fish gelatin in PBS). Sections were incubated with anti-Tctex-1 antibody diluted in blocking buffer at 4°C for ~60 hr and washed once in PBS and twice in IgG-gold buffer (0.1% ovalbumin, 0.5% cold water fish gelatin, 0.01% Tween 20, 0.5 M NaCl in 10 mM phosphate buffer [pH 7.3]). The sections were incubated for 2 hr with goat anti-rabbit IgG conjugated to 1.4 nm nanogold (Nanoprobes, Stony Brook, NY) diluted in IgG-gold buffer. Washed sections were postfixed in 2% glutaraldehyde for 10 min, washed and air dried, and the nanogold labeling silver enhanced (Danscher, 1981). The grids were then washed in H$_2$O and stained with lead citrate and 2% ethanolic uranyl acetate prior to analysis in a Zeiss EM 912Ω electron microscope.

For double labeling, sections were incubated in a mixture of anti-Tctex-1 and anti-rhodopsin antibodies in blocking buffer. After washing, sections were incubated in a mixture of goat anti-rabbit and goat anti-mouse secondary antibodies conjugated to 10 nm colloidal gold and 1.4 nm nanogold or vice versa, diluted in IgG-gold buffer. Double-labeled sections were silver enhanced for 20 min.

References

Adamus, G., Arendt, A., Zam, Z.S., McDowell, J.H., and Hargrave, P.A. (1988). Use of peptides to select for anti-rhodopsin antibodies with desired amino acid sequence specificities. Peptide Res. *1*, 42–47.

Bauch, A., Campbell, K.S., and Reth, M. (1998). Interaction of the CD5 cytoplasmic domain with the Ca2$^+$/calmodulin-dependent kinase IId. Eur. J. Immunol. *28*, 2167–2177.

Beech, P.L., Pagh-Roehl, K., Noda, Y., Hirokawa, N., Burnside, B., and Rosenbaum, J.L. (1996). Localization of kinesin superfamily proteins to the connecting cilium of fish photoreceptors. J. Cell Sci. *109*, 889–897.

Besharse, J.C., and Wetzel, M.G. (1995). Immunocytochemical localization of opsin in rod photoreceptors during periods of rapid disc assembly. J. Neurocytol. *24*, 371–388.

Breeden, L., and Nasmyth, K. (1985). Regulation of the yeast HO gene. Cold Spring Harbor Symp. Quant. Biol. *50*, 643–650.

Campbell, K.S., Cooper, S., Dessing, M., Yates, S., and Buder, A. (1998). Interaction of p59^{fyn} kinase with the dynein light chain, Tctex-1, and colocalization during cytokinesis. J. Immunol. *161*, 1728–1737.

Chang, G.-Q., Hao, Y., and Wong, F. (1993). Apoptosis: final common pathway of photoreceptor death in *rd*, *rds*, and rhodopsin mutant mice. Neuron *11*, 595–605.

Chuang, J.-Z., and Sung, C.-H. (1998). The cytoplasmic tail of rhodopsin acts as a novel apical sorting signal in polarized MDCK cells. J. Cell Biol. *142*, 1245–1256.

Collins, C.A., and Vallee, R.B. (1987). Temperature-dependent reversible assembly of taxol-treated microtubules. J. Cell Biol. *105*, 2847–2854.

Collins, C.A., and Vallee, R.B. (1989). Preparation of microtubules

from rat liver and testis: cytoplasmic dynein is a major microtubule associated protein. Cell Motil. Cytoskeleton 14, 491–500.

Corthésy-Theulaz, I., Pauloin, A., and Pfeffer, S.R. (1992). Cytoplasmic dynein participates in the centrosomal localization of the Golgi complex. J. Cell Biol. 118, 1333–1345.

Danscher, G. (1981). Histochemical demonstration of heavy metals: a revised version of the sulphide silver method suitable for both light and electron microscopy. Histochemistry 71, 1–16.

Deretic, D., and Papermaster, D.S. (1991). Polarized sorting of rhodopsin on post-Golgi membranes in frog retinal photoreceptor cells. J. Cell Biol. 113, 1281–1293.

Deretic, D., Schmerl, S., Hargrave, P.A., Arendt, A., and McDowell, J.H. (1998). Regulation of sorting and post-Golgi trafficking of rhodopsin by its C-terminal sequence QVS(A)PA. Proc. Natl. Acad. Sci. USA 95, 10620–10625.

Dillman, J.F., and Pfister, K.K. (1994). Differential phosphorylation in vivo of cytoplasmic dynein associated with anterogradely moving organelles. J. Cell Biol. 127, 1671–1681.

Dryja, T.P., and Li, T. (1995). Molecular genetics of retinitis pigmentosa. Hum. Mol. Genet. 4, 1739–1743.

Dryja, T.P., McGee, T.L., Hahn, L.B., Cowley, G.S., Olsson, J.E., Reichel, E., Sandberg, M.A., and Berson, E.L. (1990). Mutations within the rhodopsin gene in patients with autosomal dominant retinitis pigmentosa. N. Engl. J. Med. 323, 1302–1307.

Dryja, T.P., Hahn, L.B., Cowley, G.S., McGee, T.L., and Berson, E.L. (1991). Mutation spectrum of the rhodopsin gene among patients with autosomal dominant retinitis pigmentosa. Proc. Natl. Acad. Sci. USA 88, 9370–9374.

Echeverri, C.J., Paschal, B.M., Vaughan, K.T., and Vallee, R.B. (1996). Molecular characterization of the 50-kD subunit of dynactin reveals function of the complex in chromosome alignment and spindle organization during mitosis. J. Cell Biol. 132, 617–633.

Gill, S.R., Cleveland, D.W., and Schroer, T.A. (1994). Characterization of DLC-A and DLC-B, two families of cytoplasmic dynein light chain subunits. Mol. Biol. Cell 5, 645–654.

Hargrave, P.A., McDowell, J.H., Curtis, D.R., Fong, S.-L., and Juszczak, E. (1982). Preparation of peptides from bovine rhodopsin. Methods Enzymol. 81, 251–256.

Harrison, A., Olds-Clarke, P., and King, S.M. (1998). Identification of the t complex-encoded cytoplasmic dynein light chain Tctex-1 in inner arm I1 supports the involvement of flagellar dyneins in meiotic drive. J. Cell Biol. 140, 1137–1147.

Hyman, A.A. (1991). Preparation of marked microtubules for the assay of the polarity of microtubule-based motors by fluorescence. J. Cell Sci. Supp. 14, 125–127.

Karki, S., and Holzbaur, E.L. (1995). Affinity chromatography demonstrates a direct binding between cytoplasmic dynein and the dynactin complex. J. Biol. Chem. 270, 28806–28811.

King, S.M., Barbarese, E., Dillman, J.F.I., Patel-King, R.S., Carson, J.H., and Pfister, K.K. (1996a). Brain cytoplasmic and flagellar outer arm dyneins share a highly conserved Mr 8000 light chain. J. Biol. Chem. 271, 19358–19366.

King, S.M., Dillman, J.F., III, Benashski, S.E., Lye, R.J., Patel-King, R.S., and Pfister, K.K. (1996b). The mouse t-complex-encoded protein Tctex-1 is a light chain of brain cytoplasmic dynein. J. Biol. Chem. 271, 32281–32287.

King, S.M., Barbarese, E., Dillman, J.F., Benashski, S.E., Do, K.T., Patel-King, R.S., and Pfister, K.K. (1998). Cytoplasmic dynein contains a family of differentially expressed light chains. Biochemistry 37, 15033–15041.

Krebs, W., and Kühn, H. (1977). Structure of isolated bovine rod outer segment membranes. Exp. Eye Res. 25, 511–526.

Lacey, M.L., and Haimo, L.T. (1994). Cytoplasmic dynein binds to phospholipid vesicles. Cell Motil. Cytoskeleton 28, 205–212.

Lader, E., Ha, H.-S., O'Neill, M., Artzt, K., and Bennett, D. (1989). tctex-1: a candidate gene family for a mouse t-complex sterility locus. Cell 58, 969–979.

Li, Z.Y., Wong, F., Chang, J.H., Possin, D.E., Hao, Y., Petters, R.M., and Milam, A.H. (1998). Rhodopsin transgenic pigs as a model for human retinitis pigmentosa. Invest. Opthalmol. Vis. Sci. 39, 808–819.

Liu, X., Vansant, G., Udovichenko, I.P., Wolfrum, U., and Williams, D.S. (1997). Myosin VIIa, the product of the Usher 1B syndrome gene, is concentrated in the connecting cilia of photoreceptor cells. Cell Motil. Cytoskeleton 37, 240–252.

Macke, J.P., Davenport, C.M., Jacobson, S.G., Hennessey, J.C., Gonzalez-Fernandez, F., Conway, B.P., Heckenlively, J., Palmer, R., Maumenee, I.H., Sieving, P., et al. (1993). Identification of novel rhodopsin mutations responsible for retinitis pigmentosa: implications for the structure and function of rhodopsin. Am. J. Hum. Genet. 53, 80–89.

McGrail, M., Gepner, J., Silvanovich, A., Ludmann, S., Serr, M., and Hays, T.S. (1995). Regulation of cytoplasmic dynein function in vivo by the Drosophila Glued complex. J. Cell Biol. 131, 411–425.

Molday, R.S., and MacKenzie, D. (1983). Monoclonal antibodies to rhodopsin: characterization, cross-reactivity and application as structural probes. Biochemistry 22, 653–660.

Mou, T., Kraas, J.R., Fung, E.T., and Swope, S.L. (1998). Identification of a dynein molecular motor component in Torpedo electroplax; binding and phosphorylation of Tctex-1 by Fyn. FEBS Lett. 435, 275–281.

Muresan, V., Godek, C.P., Reese, T.S., and Schnapp, B.J. (1996). Plus-end motors override minus-end motors during transport of squid axon vesicles on microtubules. J. Cell Biol. 135, 383–397.

Nagano, F., Orita, S., Sasaki, T., Naito, A., Sakaguchi, G., Maeda, M., Watanabe, T., Kominami, E., Uchiyama, Y., and Takai, Y. (1998). Interaction of Doc2 with tctex-1, a light chain of cytoplasmic dynein. Implications for dynein-dependent vesicle transport. J. Biol. Chem. 273, 30065–30068.

Papermaster, D.S., Schneider, B.G., Defoe, D., and Besharse, J.C. (1986). Biosynthesis and vectorial transport of opsin on vesicles in retinal rod photoreceptors. J. Histochem. Cytochem. 34, 5–16.

Paschal, B.M., Shpetner, H.S., and Vallee, R.B. (1987). MAP 1C is a microtubule-activated ATPase which translocates microtubules in vitro and has dynein-like properties. J. Cell Biol. 105, 1273–1282.

Pfister, K.K., Salata, M.W., Dillman, J.F., Torre, E., and Lye, R.J. (1996). Identification and developmental regulation of a neuron-specific subunit of cytoplasmic dynein. Mol. Biol. Cell 7, 331–343.

Plamann, M., Minke, P.F., Tinseley, J.H., and Bruno, K.S. (1994). Cytoplasmic dynein and actin-related protein Arp1 are required for normal nuclear distribution in filamentous fungi. J. Cell Biol. 127, 139–149.

Portera-Cailliau, C., Sung, C.-H., Nathans, J., and Adler, R. (1994). Apoptotic photoreceptor cell death in mouse models of retinitis pigmentosa. Proc. Natl. Acad. Sci. USA 91, 974–978.

Rohlich, P. (1975). The sensory cilium of retinal rods is analogous to the transitional zone of motile cilia. Cell Tissue Res. 161, 421–430.

Roux, A.-F., Rommens, J., McDowell, C., Anson-Cartwright, L., Bell, S., Schappert, K., Fishman, G.A., and Musarella, M. (1994). Identification of a gene from Xp21 with similarity to the tctex-1 gene of the murine t complex. Hum. Mol. Genet. 3, 257–263.

Schroer, T.A., and Sheetz, M.P. (1991). Two activators of microtubule-based vesicle transport. J. Cell Biol. 115, 1309–1318.

Smith, H.G., Stubbs, G.W., and Litman, B.J. (1975). The isolation and purification of osmotically intact discs from retinal rod outer segments. Exp. Eye Res. 20, 211–217.

Spencer, M., Detwiler, P.B., and Bunt-Milam, A.H. (1988). Distribution of membrane proteins in mechanically dissociated retinal rods. Invest. Ophthalmol. Vis. Sci. 29, 1012–1020.

Steffen, W., Karki, S., Vaughan, K.T., Vallee, R.B., Holzbaur, E.L.F., Weiss, D.G., and Kuznetsov, S.A. (1997). The involvement of the intermediate chain of cytoplasmic dynein in binding the motor complex to membranous organelles of Xenopus oocytes. Mol. Biol. Cell 8, 2077–2088.

Steuer, E.R., Wordeman, L., Schroer, T.A., and Sheetz, M.P. (1990). Localization of cytoplasmic dynein to mitotic spindles and kinetochores. Nature 345, 266–268.

Sung, C.-H., Davenport, C.M., Hennessey, J.C., Maumenee, I.H., Jacobson, S.G., Heckenlively, J.R., Nowakowski, R., Fishman, G., Gouras, P., and Nathans, J. (1991a). Rhodopsin mutations in autosomal dominant retinitis pigmentosa. Proc. Natl. Acad. Sci. USA 88, 6481–6485.

Sung, C.-H., Schneider, B.G., Agarwal, N., Papermaster, D.S., and Nathans, J. (1991b). Functional heterogeneity of mutant rhodopsins responsible for autosomal dominant retinitis pigmentosa. Proc. Natl. Acad. Sci. USA *88*, 8840–8844.

Sung, C.-H., Davenport, C.M., and Nathans, J. (1993). Rhodopsin mutations responsible for autosomal dominant retinitis pigmentosa: clustering of functional classes along the polypeptide chain. J. Biol. Chem. *268*, 26645–26649.

Sung, C.-H., Makino, C., Baylor, D., and Nathans, J. (1994). A rhodopsin gene mutation responsible for autosomal dominant retinitis pigmentosa results in a protein that is defective in localization to the photoreceptor outer segment. J. Neurosci. *14*, 5818–5833.

Tai, A.W., Chuang, J.-Z., and Sung, C.-H. (1998). Localization of Tctex-1, a cytoplasmic dynein light chain, to the Golgi apparatus and evidence for dynein complex heterogeneity. J. Biol. Chem. *273*, 19639–19649.

Troutt, L.L., and Burnside, B. (1988). Microtubule polarity and distribution in teleost photoreceptors. J. Neurosci. *8*, 2371–2380.

Vallee, R.B., Vaughan, K.T., and Echeverri, C.J. (1995). Targeting of cytoplasmic dynein to membranous organelles and kinetochores via dynactin. Cold Spring Harbor Symp. Quant. Biol. *50*, 803–811.

Vaughan, K.T., and Vallee, R.B. (1995). Cytoplasmic dynein binds dynactin through a direct interaction between the intermediate chains and p150*Glued*. J. Cell Biol. *131*, 1507–1516.

Wang, Z., Khan, S., and Sheetz, M.P. (1995). Single cytoplasmic dynein molecule movements: characterization and comparison with kinesin. Biophys. J. *69*, 2011–2023.

Watanabe, T.K., Fujiwara, T., Shimizu, F., Okuno, S., Suzuki, M., Takahashi, E., Nakamura, Y., and Hirai, Y. (1996). Cloning, expression, and mapping of TCTEL1, a putative human homologue of murine *Tcte1*, to 6q. Cytogenet. Cell Genet. *73*, 153–156.

Weiss, E.R., Hao, Y., Dickerson, C.D., Osawa, S., Shi, W., Zhang, L., and Wong, F. (1995). Altered cAMP levels in retinas from transgenic mice expressing a rhodopsin mutant. Biochem. Biophys. Res. Commun. *216*, 755–761.

Wolfrum, U. (1995). Centrin in the photoreceptor cells of mammalian retinae. Cell Motil. Cytoskeleton *32*, 55–64.

Young, R.W. (1976). Visual cells and the concept of renewal. Invest. Ophthalmol. Vis. Sci. *15*, 700–725.